Hindawi Publishing Corporation
International Journal of Distributed Sensor Networks
Volume 2013, Article ID 475761, 9 pages
http://dx.doi.org/10.1155/2013/475761

Research Article

SDMA-Based Aeronautical Machine-to-Machine Communications under SINR Constraints

Jindong Xie, Lin Bai, Jun Zhang, and Tao Zhang

School of Electronic and Information Engineering, Beihang University, Beijing 100191, China

Correspondence should be addressed to Lin Bai; l.bai@buaa.edu.cn

Received 13 August 2013; Accepted 18 November 2013

Academic Editor: Jianhua He

In order to achieve an efficient usage on a limited spectrum for aeronautical machine-to-machine (M2M) communications, in this paper, a space division multiple access- (SDMA-) based architecture is proposed, where the random access of short messages noisy (SMN) M2M communications is considered between autopilot systems onboard and the ground control center for the air traffic precise control, that is, full 4-dimensional trajectory management. It shows that using a zero-forcing beamforming combined with a low complexity aircraft grouping strategy, the SDMA-based mechanism is able to improve the spectrum efficiency under signal to interference plus noise ratio (SINR) constraints.

1. Introduction

To ensure the continuous safety and efficiency improvement of air traffic flows, the accurate trajectory surveillance and control abilities are highly required for the advanced air traffic control (ATC), that is, 4-dimensional trajectory- (4DT-) based management (The "4D-trajectory management" concept improves the ATC by using "time" with early traffic sequencing based on the aircrafts way-point passage predictions. It is planned to be deployed from 2017 and allowed to enter into services beyond 2020), which has already been scheduled and will be employed in the following decade [1, 2]. Therefore, the future air to ground (A/G) datalink is foreseen to support continuous interactions between the flight management system (FMS) onboard and the ground ATC system for real-time automatic monitoring and control [3–6]. Since an ATC message payload generally contains only hundreds of bits (e.g., position coordinates and timestamps) [7] and needs to be updated frequently (e.g., 16 times per second) [8, 9], future aeronautical communications can be considered as typical short messages noisy (SMN) machine-to-machine (M2M) communications.

In order to support 4DT services, the next generation aeronautical datalinks will be developed by taking into account the SMN-M2M communications. For the sake of safety-of-life related issues [10], two crucial characteristics have to be considered as follows:

(i) all aircraft should maintain seamless connections with the control center;

(ii) each connection has to support a primary rate for real-time interactions.

Here, a primary rate is defined as the basic achievable data rate to provide essential communication services for 4DT management.

Unfortunately, the existing aeronautical datalinks may not be able to satisfy both two objectives from above efficiently [11, 12]. On the other hand, considering the limited aeronautical spectrum [13], the spectrum efficient strategy of aeronautical M2M communications can be reconfigured under the primary rate constraint. In summary, the future aeronautical M2M communication system can be demonstrated as follows:

(i) a spectrum should be reused by multiple airborne station (AS) nodes;

(ii) aircraft could transmit or receive short messages at real time, without extra resource allocations;

(iii) a primary rate should be guaranteed for reliable M2M communications.

Since an interval in distance has to be guaranteed between different aircrafts (e.g., 4~8 nautical miles separation along with a flight course [14]), space division multiple access (SDMA) could be an efficient means [15, 16] to improve the aeronautical spectrum efficiency. Based on SDMA, a spectrum will be multiplexed by multiple AS nodes naturally. Also, real-time A/G interactions could be supported by SDMA assisted random access. With the help of SDMA, potential conflicts of random access will be mitigated easily.

In particular, beamforming over multiple-antenna systems can be an efficient approach to perform the SDMA [17]. Among different beamforming techniques, dirty paper coding (DPC) [18] has been developed to provide the optimal performance by separating combined spatially selective signals. However, DPC is impractical due to its prohibitively high complexity.

As a low complexity linear beamforming approach, orthogonal beamforming [19] is able to support hierarchical priority guaranteed SDMA in M2M communications over cellular networks [20], while it may not be appropriate for aeronautical SMN-M2M communications as an equal, performance of different 4DT management services is required on safety-of-life level. Combined with a semiorthogonal users selection (SUS) scheme [21], zero-forcing beamforming (ZFBF) has been proposed in [22] to provide equitable performance for all selected users. Thus, we may consider ZFBF as a good candidate technique for SDMA-based aeronautical M2M communications. However, unfortunately, SUS cannot achieve the SNR or rates to a certain desired level at each iteration of user selection. Therefore, ZFBF-SUS cannot guarantee the reliability of connections with the safety-of-life related 4DT management.

In this paper, we propose an SDMA-based approach for the future L-band continental A/G communication systems [23, 24]. By using ZFBF over antenna arrays equipped in a ground station (GS), one frequency spectrum is able to support M2M random accesses without conflicts for multiple AS nodes, simultaneously. Moreover, in order to guarantee the primary rate for A/G communications, we propose a low complexity user selection strategy for the ZFBF under signal to interference plus noise ratio (SINR) constraints to exploit the SDMA gain.

The rest of the paper is organized as follows. Section 2 provides the system model. Our proposed SDMA-based mechanism for aeronautical M2M communications is introduced in Section 3. After the impacts of feedback reliability discussion in Section 4, the simulation results are presented in Section 5 to analyze the performance. Finally, we conclude this paper in Section 6.

Notation. The superscripts T and H stand for the transpose and Hermitian transpose, respectively. Denote by $\|\cdot\|$ the 2-norm, and $|\cdot|$ is the total elements number of a certain set. The statistical expectation is represented by $\mathbb{E}[\cdot]$. The distribution of a circularly symmetric complex Gaussian (CSCG) random variable with mean a and covariance b is denoted by $\mathcal{CN}(a, b)$. Besides, $\mathbf{I}_{(M\times N)}$ stands for an $M \times N$ identity matrix, and $\mathbf{I}_M = \mathbf{I}_{(M\times M)}$.

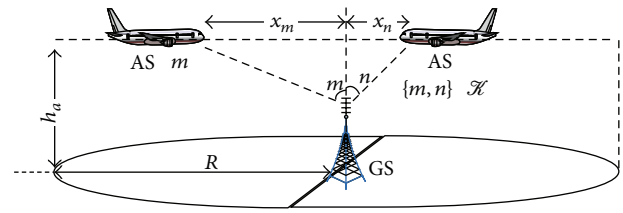

Figure 1: The geometry model for A/G communications over the GS equipped with multiple antennas array in a macrocell.

2. System Model

Consider a section of the continental A/G communication system with K aircraft randomly located in a macrocell. Let $\mathcal{K} = \{1, 2, \ldots, K\}$ be the index set of all AS nodes. We suppose that each AS is equipped with a single antenna, while the GS is equipped with a uniform linear array (ULA) of M elements. Due to the reciprocity, we only focus on the reverse link of A/G communications (i.e., from AS to GS), while the main results are easily extended to forward link scenarios.

Let the index of a certain spectrum be $f \in \mathcal{F} = \{1, 2, \ldots, F\}$ with $F \leq K$. Assume that AS-m and AS-n are assigned as a group to access the fth spectrum, simultaneously. The resulting geometry model can be described in Figure 1.

Let $\Theta_{\mathcal{S}_f} = \{\theta_m, \theta_n\}$ represent the angle of arrival (AoA) set of AS-m and AS-n with respect to the array normal, where $\mathcal{S}_f = \{m, n\}$ denotes the set of all selected AS nodes in group f. For the sake of simplicity, we do not consider the effect of azimuth angles in the paper, since the ULA is a 2-dimensional distinguish array and insensitive to the azimuth angle (A 3-dimensional distinguish array such as a circular or planar array can be considered as an extension of this work, where the azimuth angles are taken into account).

In aeronautical A/G communication scenario, a wireless channel is generally characterized by a Rician fading with a strong line of sight (LoS) component and a weak diffusion path [25, 26]. If the Rician factor is given by $K_{\text{Rice}} = 15\,\text{dB}$ in a typical en-route scenario [24], the contribution of LoS component becomes far greater than that of the diffusion part. Consequently, an additive white Gaussian noise (AWGN) LoS channel can be used to sketch the A/G channel, which is further modeled as an array response vector (ARV) since an antenna array is employed at the GS.

Considering all M elements of the ULA are placed at the direction of $\mathcal{X}$-axis, the ARV of the AS-m is given by

$$\mathbf{a}_m = \mathbf{a}(\theta_m) = \begin{bmatrix} 1 \\ e^{-j2\pi(d/\lambda)\cos\theta_m} \\ \vdots \\ e^{-j2\pi(M-1)(d/\lambda)\cos\theta_m} \end{bmatrix}, \quad (1)$$

where d is the antenna spacing and λ denotes the wavelength of the carrier. Since AoAs of AS nodes could be seen unchanged within a short period and can be easily obtained

from positioning systems or efficient AoA estimations, it can be assumed that the ARV of each AS is constant over the duration of a time slot and is well known by the GS.

Denote by $N_f = |\mathcal{S}_f|$ is the total number of selected AS nodes on the fth spectrum resource, for example, $N_f = 2$ in Figure 1. Moreover, we have $\mathcal{S}_1 \cup \cdots \mathcal{S}_f \cdots \cup \mathcal{S}_F = \mathcal{K}$ and $N_1 + \cdots + N_f + \cdots + N_F = K$, where F is the total number of required frequency resources.

Let $\mathbf{H}_{\mathcal{S}_f} = [\mathbf{a}_m, \mathbf{a}_n] \in \mathcal{C}^{M \times N_f}$ and let $\mathbf{S}_{\mathcal{S}_f} = [s_m, s_n]^T \in \mathcal{C}^{N_f \times 1}$ be the channel matrix and expected signal vector from AS nodes in $\mathcal{S}_f$ to GS, respectively. Then the received signal vector $\mathbf{y}_f$ at the GS over spectrum f is given by

$$\mathbf{y}_f = \mathbf{H}_{\mathcal{S}_f} \mathbf{S}_{\mathcal{S}_f} + \mathbf{z}_f, \tag{2}$$

where $\mathbf{z}_f$ is the additive white Gaussian noise and $\mathbf{z}_f \sim \mathcal{CN}(0, \sigma^2 \mathbf{I}_{N_f})$.

The transmission power of s_i from AS-i is assumed to be identical for different i; that is, $\mathbb{E}[|s_i|^2] = P_t$. However, due to the propagation path loss, the received powers could be different. Since the channels between AS and GS include strong LoS components, for the sake of simplicity, the received power can be described using the following simple path-loss model [27]:

$$\frac{1}{\gamma} = \frac{P_t}{P_r} = \left(\frac{4\pi l_0}{\lambda}\right)^2 \left(\frac{l}{l_0}\right)^n, \tag{3}$$

where P_t and P_r denote transmit and receive power, respectively. In (3), λ is propagation wavelength, n is the path-loss exponent, l is the distance between the transmitter and receiver, and l_0 is a close-in reference distance. Since λ, n, and l_0 are considered as constants, the path-loss is a function of l with the known parameters λ, n, and l_0.

3. Primary Rate Guaranteed SDMA

In this section, the main solution of SDMA-based mechanism for aeronautical M2M communications is presented. As aforementioned, antenna array beamforming and multiple users selection are coupled issues. Lets first consider the beamforming problem.

3.1. Zero-Forcing Beamforming. Let

$$\begin{aligned} \mathbf{W}_f &= \left[\mathbf{w}_1, \mathbf{w}_2, \ldots, \mathbf{w}_{N_f}\right] \\ &= \left[\frac{\widetilde{\mathbf{w}}_1}{\|\widetilde{\mathbf{w}}_1\|}, \frac{\widetilde{\mathbf{w}}_2}{\|\widetilde{\mathbf{w}}_2\|}, \ldots, \frac{\widetilde{\mathbf{w}}_{N_f}}{\|\widetilde{\mathbf{w}}_{N_f}\|}\right], \end{aligned} \tag{4}$$

where $\widetilde{\mathbf{w}}_i$ is the ith column vector of $\mathbf{H}_{\mathcal{S}_f}(\mathbf{H}_{\mathcal{S}_f}^{\mathrm{H}} \mathbf{H}_{\mathcal{S}_f})^{-1}$, that is, the Hermitian transpose of the Moore-Penrose pseudoinverse of $\mathbf{H}_{\mathcal{S}_f}$.

Since $\mathbf{W}_f$ is generated by the pseudoinverse of $\mathbf{H}_{\mathcal{S}_f}^{\mathrm{H}}$, the column vector $\mathbf{w}_i$ in $\mathbf{W}_f$ becomes orthogonal with the column vectors $\mathbf{a}_j$ in $\mathbf{H}_{\mathcal{S}_f}$, when $i \neq j$ and $1 \leq \{i, j\} \leq N_f$. According to Figure 2, the estimated signal of the ith selected user in $\mathcal{S}_f$ is given by

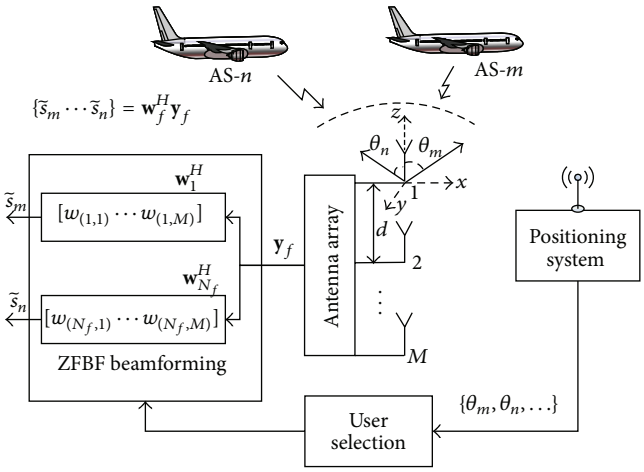

Figure 2: The ZFBF beamforming for A/G communications.

$$\widetilde{s}_i = \mathbf{w}_{k_i}^{\mathrm{H}} \mathbf{y}_f = \frac{\sqrt{\gamma_{k_i} P_t}}{\|\widetilde{\mathbf{w}}_i\|} s_i, \tag{5}$$

where γ_k is the path-loss parameter in (3) with respect to AS-k. Besides, $1/\|\widetilde{\mathbf{w}}_i\|$ is termed as equivalent channel gain (ECG). The received SINR expression of the ith selected user in $\mathcal{S}_f$ can be described as

$$\mathrm{SINR}_{k_i} = \frac{\gamma_{k_i} P_t}{\|\widetilde{\mathbf{w}}_i\|^2 \sigma^2}, \tag{6}$$

where $k_i \in \mathcal{K}$ is the index of the ith selected AS in $\mathcal{S}_f$. Then the achievable rate of AS-k_i is given by

$$r_{k_i} = \log_2\left(1 + \frac{\gamma_{k_i} P_t}{\|\widetilde{\mathbf{w}}_i\|^2 \sigma^2}\right). \tag{7}$$

Since ATC services are safety-of-life related, the proposed system should be able to provide a primary rate for each selected AS node. Here, the primary rate is defined as

$$\overline{r} = \log_2\left(1 + \overline{\mathrm{SNR}}\right), \tag{8}$$

where $\overline{\mathrm{SNR}}$ is the threshold SNR of an edge-located AS node without performing the SDMA. Then SINR constraints can be applied to all selected AS nodes as follows:

$$\begin{aligned} r_{k_i} &\geq \overline{r}, \\ \mathrm{SINR}_{k_i} &\geq \overline{\mathrm{SNR}}. \end{aligned} \tag{9}$$

By taking into account the path loss in a macrocell, assuming all the AS have the same noise variance (i.e., $\sigma^2 = 1$), the threshold transmitting power is obtained by

$$\overline{P}_t = \left(\frac{4\pi l_0}{\lambda}\right)^2 \left(\frac{R}{l_0}\right)^n \overline{\mathrm{SNR}}, \tag{10}$$

where $\overline{\mathrm{SNR}}$, R, l_0, λ, and n are given.

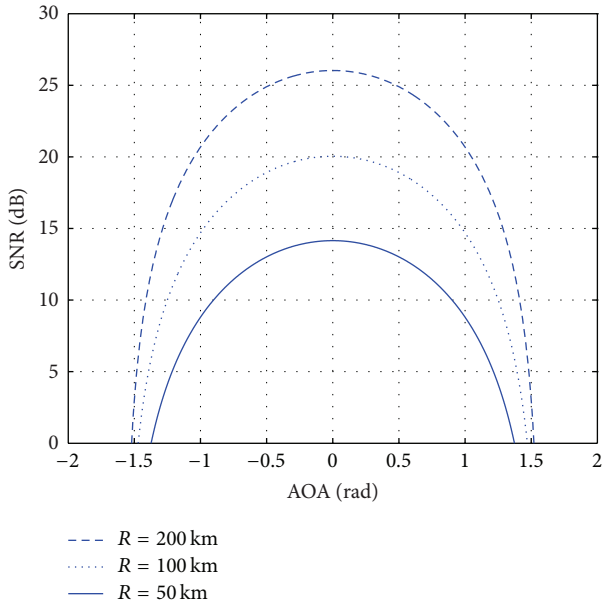

FIGURE 3: The received SNR with $\overline{P}_t$ transmitting power versus various potential AoAs, where $\overline{\text{SNR}} = 0$ dB, $l_0 = 1$ m, $\lambda = 0.3$ m, and $n = 2.0$.

Apparently, $\overline{P}_t$ is essential and desired by all AS transmitters, since each AS always fights over the edge of a macrocell. However, if one AS transmits signals using power of $P_t = \overline{P}_t$, the received SNR, which is affected by the path loss, can be described in Figure 3.

As Figure 3 illustrates, the received SNR of AS nodes with smaller absolute AoAs is higher than those nodes located at the edge area of a macrocell. Since $\overline{\text{SNR}}$ is sufficiently large to hold the primary rate, the higher received SNR of inner AS nodes becomes unnecessary with respect to supporting the 4DT management services. Therefore, the conventional power control schemes have shown the disadvantages for the sake of the spectral efficiency.

Using ZFBF, a spectrum can be multiplexed among inner and fringe AS nodes. In order to measure the advantage of ZFBF-SDMA, the improvement of performance can be described as an SDMA gain [28–30]. Let the SDMA gain be the ratio of the spectrum efficiency with and without the SDMA applied. If the primary rate constraint of M2M communications for different aircraft is identical and represented by $\overline{r}$, the SDMA gain is given by

$$G_{\text{SDMA}} = \frac{K\overline{r}/F}{K\overline{r}/K} = \frac{K}{F}. \tag{11}$$

It shows in (11) that smaller F leads to higher SDMA gain. Then it is desired to develop a user selection method to perform ZFBF-SDMA with a small F. Since positions of AS nodes (including AoAs and propagation distances) may cause significant impacts on SINR, AS nodes cannot be grouped randomly due to the SINR constraint. Therefore, the multiuser selection plays a crucial role in the primary rate guaranteed SDMA, which results in improved and reliable overall performance.

3.2. Low Complexity User Selection. The optimal user selection is the exhaustive search, which is impractical due to the prohibit high complexity. The greedy algorithms, such as semiorthogonal user selection (SUS) [22] could be efficient but suboptimal. However, since the SUS may not secure the SINR of each candidate, the primary rate or SINR constraint cannot be guaranteed. If the pseudoinverse operation is carried out on channel matrix of selected users iteratively, SNR may be traceable but the computational complexity, that is, $\mathcal{O}(KM^3)$, is considerably high for the time varying scenarios of aeronautical communications. In this subsection, we propose a low complexity user selection with complexity of $\mathcal{O}(KM^2)$, which is able to guarantee the rate or SINR constraint for different users.

In order to avoid pseudoinverse operations (which lead to high complexity) in the process of user selection, we focus on the expression of the received SINR in (6). Apparently, the best pairing candidate is to choose the one that maximize the SINR as follows:

$$k_i^* = \arg\max_{i\in\mathcal{K}} \frac{\gamma P_t}{\left\|\widetilde{\mathbf{w}}_i\right\|^2 \sigma^2}. \tag{12}$$

Note that if $\|\widetilde{\mathbf{w}}_i\|$ is obtained without taking pseudoinverse, user selection under the SINR constraint can be simplified. Next steps will illustrate the dedicated way of inverse-free user selection.

The orthonormal basis of the subspace spanned by $\mathbf{H}_{\mathcal{S}_f}$ can be generated as

$$\mathbf{g}_n = \frac{\widetilde{\mathbf{g}}_n}{\left\|\widetilde{\mathbf{g}}_n\right\|}, \quad 1 \le n \le N_f, \tag{13}$$

where N_f, $(N_f \le M)$, is the number of accepted AS nodes in Group f, and

$$\widetilde{\mathbf{g}}_n = \left[\mathbf{I}_M - \sum_{i=1}^{n-1} \frac{\widetilde{\mathbf{g}}_i \widetilde{\mathbf{g}}_i^{\text{H}}}{\left\|\widetilde{\mathbf{g}}_i\right\|^2}\right] \mathbf{a}_{k_n}. \tag{14}$$

Therefore, the channel vector of the nth selected user for the fth spectrum can be rewritten as

$$\mathbf{a}_{k_n} = \widetilde{\mathbf{g}}_n + \sum_{i=1}^{n-1} \frac{\widetilde{\mathbf{g}}_i \widetilde{\mathbf{g}}_i^{\text{H}}}{\left\|\widetilde{\mathbf{g}}_i\right\|^2} \mathbf{a}_{k_n}. \tag{15}$$

Then the channel matrix $\mathbf{H}_{\mathcal{S}}$ is decomposed as

$$\mathbf{H}_{\mathcal{S}_f} = \mathbf{QRD}. \tag{16}$$

In (16), the unitary matrix $\mathbf{Q}$ is given by

$$\mathbf{Q} = \left[\frac{\widetilde{\mathbf{g}}_1}{\left\|\widetilde{\mathbf{g}}_1\right\|}, \ldots \frac{\widetilde{\mathbf{g}}_n}{\left\|\widetilde{\mathbf{g}}_n\right\|}, \ldots, \frac{\widetilde{\mathbf{g}}_{N_f}}{\left\|\widetilde{\mathbf{g}}_{N_f}\right\|}\right]. \tag{17}$$

The upper triangular matrix $\mathbf{R}$ is given by

$$\mathbf{R} = \begin{bmatrix} 1 & \xi_{1,2} & \cdots & \xi_{1,N_f} \\ 0 & \ddots & \vdots & \vdots \\ \vdots & \vdots & 1 & \xi_{N_f-1,N_f} \\ 0 & 0 & \cdots & 1 \end{bmatrix}, \tag{18}$$

where $\xi_{i,j} = \widetilde{\mathbf{g}}_i^{\mathrm{H}}\mathbf{a}_j/(\|\widetilde{\mathbf{g}}_i\|\|\widetilde{\mathbf{g}}_j\|)$, and the diagonal matrix $\mathbf{D}$ is written as

$$\mathbf{D} = \mathrm{diag}\left[\|\widetilde{\mathbf{g}}_1\|, \ldots, \|\widetilde{\mathbf{g}}_n\|, \ldots, \|\widetilde{\mathbf{g}}_{N_f}\|\right]. \tag{19}$$

According to (4) and (6), the denominator of the SINR expression, which is directly affected by ECG, can be written as

$$\begin{aligned}\|\widetilde{\mathbf{w}}_n\|^2 &= \left(\mathbf{W}_f^{\mathrm{H}}\mathbf{W}_f\right)_{n,n} \\ &\overset{(a)}{=} \left(\mathbf{D}^{\mathrm{H}}\mathbf{R}^{\mathrm{H}}\mathbf{Q}^{\mathrm{H}}\mathbf{Q}\mathbf{R}\mathbf{D}\right)^{-1}_{n,n} \\ &\overset{(b)}{=} \left(\mathbf{D}^{\mathrm{H}}\mathbf{R}^{\mathrm{H}}\mathbf{R}\mathbf{D}\right)^{-1}_{n,n} \\ &\overset{(c)}{=} \frac{\left(\mathbf{R}^{\mathrm{H}}\mathbf{R}\right)^{-1}_{n,n}}{\|\widetilde{\mathbf{g}}_n\|^2},\end{aligned} \tag{20}$$

where $(\mathbf{X})_{i,j}$ denotes the (i,j)th element of $\mathbf{X}$. Note that equality (a) is based on the fact that $\mathbf{W}_f = \mathbf{H}_{\mathcal{S}_f}(\mathbf{H}_{\mathcal{S}_f}^{\mathrm{H}}\mathbf{H}_{\mathcal{S}_f})^{-1}$ and (16). Since $\mathbf{Q}$ is a unitary matrix; that is, $\mathbf{Q}^{\mathrm{H}}\mathbf{Q} = \mathbf{I}_M$, equality (b) can be readily obtained. Finally, equality (c) is verified by noticing that $\mathbf{D}$ is a diagonal matrix.

Besides, the numerator of (20), based on [22], can be decomposed as

$$\begin{aligned}\left(\mathbf{R}^{\mathrm{H}}\mathbf{R}\right)^{-1}_{n,n} &= \sum_{j=1}^{N}\left|\left(\mathbf{R}^{-1}\right)_{n,j}\right|^2 \\ &= \left|\left(\mathbf{R}^{-1}\right)_{n,n}\right|^2 + \sum_{j=1, j\neq n}^{N}\left|\left(\mathbf{R}^{-1}\right)_{n,j}\right|^2.\end{aligned} \tag{21}$$

In order to obtain the $\mathbf{R}^{-1}$, the $\mathbf{R}$ can be decomposed by

$$\mathbf{R}_n = \begin{bmatrix}\mathbf{R}_{n-1} & \mathbf{r}_{n-1} \\ \mathbf{0} & 1\end{bmatrix}, \tag{22}$$

where $\mathbf{R}_n$ denotes the $n \times n$ sized submatrix of $\mathbf{R}$ and $\mathbf{r}_{n-1} = [\xi_{1,n}, \ldots, \xi_{n-1,n}]^{\mathrm{T}}$. Thus, the $\mathbf{R}^{-1}$ can be readily obtained by

$$\mathbf{R}_n^{-1} = \begin{bmatrix}\mathbf{R}_{n-1}^{-1} & -\mathbf{R}_{n-1}^{-1}\mathbf{r}_{n-1} \\ \mathbf{0} & 1\end{bmatrix}. \tag{23}$$

Since $\mathbf{R}_1^{-1} = \mathbf{R}_1 = 1$ and $\mathbf{R}_n^{-1}$ is the function of $\mathbf{R}_{n-1}^{-1}$, the inverse of $\mathbf{R}$ can be calculated by taking $n-1$ iterations of vector-matrix multiplication. Note that $\mathbf{R}^{-1}$ is an upper triangular matrix and $|(\mathbf{R}^{-1})_{n,n}| = 1$, $1 \le n \le N_f$. Hence, the received SINR of the nth selected user $k_n \in \mathcal{S}_f$ can be rewritten as

$$\mathrm{SINR}_{k_n} = \frac{\gamma_{k_n}P_t}{\sigma^2}\frac{\|\widetilde{\mathbf{g}}_n\|^2}{\left(1 + \sum_{j=n+1}^{N_f}\left|(\mathbf{R}^{-1})_{n,j}\right|^2\right)}. \tag{24}$$

It is shown that the denominator of (24) can be obtained only by taking vectors multiplication. Based on (24), the matrix-inverse free selection (MFS) for all K AS nodes is summarized in Algorithm 1.

Based on steps {5, 7, and 9} in Algorithm 1, it is easy to observe that the complexity of proposed MFS is $\mathcal{O}(KM^2)$, which is one order lower than those with matrix-inverse on each iteration, that is, $\mathcal{O}(KM^3)$. From steps 15~19, it shows that the received SINR of all accepted AS nodes have to be larger than $\overline{SNR}$, where the SINR constraints are confirmed for all selected AS nodes, that is, a reliable SDMA for spectrum multiplexing.

4. Impacts of AoA Reliability

So far, we have assumed that perfect AoA information can be obtained at the GS and the AoAs is unchanged within a short time slot. However, the AoAs actually change during the path of AS nodes flying over the GS. Since imperfect AoAs can seriously influence the SDMA performance, impacts of the AoA reliability (i.e., AoA accuracy and updating frequency) will be discussed in this section.

4.1. The Imperfect AoA Estimation. Note that any error or inaccurate AoA estimation will result in a degraded beamforming performance and lead to the interference in 4DT A/G data transmission, which is not desirable. It is important to investigate the impact of imperfect AoA estimations on the performance of the proposed aeronautical SDMA architecture.

While AoA estimation errors have been studied in the literature [31–33], analytical formulations to see the impact of AoA estimation errors are difficult for multiple user broadcasting with SDMA. Thus, in this section, we present a preliminary simulation result on the sensitivity of sum rates to imperfect AoAs. The estimated AoA by the GS, denoted by $\widehat{\theta}$, can be characterized as a random variable with a uniform distribution as follows [31]:

$$f\left(\widehat{\theta}\right) = \frac{1}{2\Delta}, \quad -\Delta \le \left(\widehat{\theta} - \theta\right) \le \Delta, \tag{25}$$

where θ is the true AoA and Δ^2 is the variance of the AoA estimation error in $\widehat{\theta}$. Let Δ be normalized as $\Delta = \tau\Delta_{\max}$, where τ is the proportionality factor and $\Delta_{\max}$ is the maximum AoA error obtained by the maximum null-to-null beam width (i.e., from null-to-null at the both sides of the $\theta_m = 90^\circ$). Based on (1) and the array factor expression of ULA in [16], $\Delta_{\max}$ can be found as

$$\Delta_{\max} = 0.5\pi - \arccos\left(\frac{2}{M}\right). \tag{26}$$

We can evaluate the impact of imperfect AoA information by defining SINR degradation as

$$\delta_{\mathrm{SINR}} = \mathrm{SINR}\left(\widehat{\theta}\right) - \mathrm{SINR}\left(\theta\right). \tag{27}$$

In (27), $\mathrm{SINR}(\widehat{\theta})$ denotes the degraded SINR, which is obtained by beamforming with $\widehat{\theta}$, and $\mathrm{SINR}(\theta)$ means the ideal result with θ. Then, the average SINR degradation can be found in Figure 4.

Input: $\{\mathbf{A}, \mathbf{H}, K, M, \overline{\text{SNR}}, \overline{P}_t\}$
(1) $f = 1$;
(2) **while** $f < K$ **do**
(3) $k_1 = \arg\min(\text{abs}(\mathbf{A}))$;
(4) $\mathbf{H}_{S_f} = \mathbf{H}(:, k_1)$;
(5) **for** $i = 2 : M$
(6) Generate $\mathbf{g}_{i-1}$ by (13);
(7) **for** $k = 1 : K$
(8) Generate $\mathbf{R}_i$ by (18);
(9) **for** $j = 1 : i - 1$
(10) Generate $\mathbf{R}_j^{-1}$ by (23);
(11) **end for** j
(12) Calculate $\text{SINR}(k_i)$ by (24);
(13) **end for** k
(14) $k_i^* = \arg\max \text{SINR}(k_i)$;
(15) **if** $\text{SINR}(k_i^*) > \overline{\text{SNR}}$
(16) $\mathbf{H}_{S_f} = [\mathbf{H}_{S_f}, \mathbf{H}(:, k_i^*)]$;
(17) **else**
(18) **break**;
(19) **end if**
(20) **end for** i
(21) $f = f + 1$;
(22) **end while**
(23) $F = f$;
Output: $\{F, \{\mathbf{H}_{S_1}, \ldots, \mathbf{H}_{S_F}\}\}$

Algorithm 1: The matrix-inverse free selection: **MFS**.

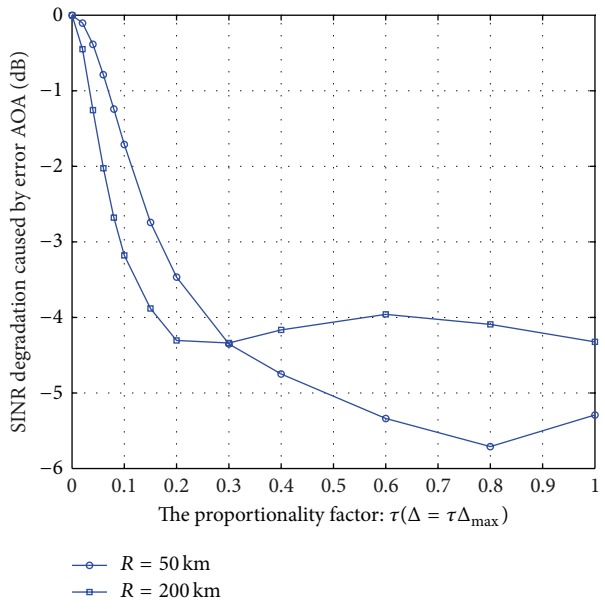

Figure 4: Average SINR degradation as a function of τ, where $M = 10$ and $K = 50$.

As shown in Figure 4, the δ_{SINR} decreases with Δ up to $\Delta_{\max}$, which results from the fact that the proposed SDMA highly depends on the phase accuracy of ARVs. Although a noticeable mitigation of the performance loss can been seen at the case of a large AoA error, the overall degradation of SINR is unacceptable. Therefore, in order to provide a reliable A/G communication service, the GS has to obtain AoA information of all AS nodes precisely.

If the AoA information is obtained over AS feedback, the updating frequency will be crucial considering the position of an aircraft changes rapidly. This issue will discuss in the next subsection.

4.2. AoA Update Frequency. In the implementation of the primary rate guaranteed SDMA, it is possible to obtain the positions or flight tracks of all AS nodes by AS feedback or positioning function of the ATC system. Consequently, the frequency of information update will affect the AoA accuracy directly and be discussed in this subsection.

Based on the geographic model in Figure 1, the AoA of an AS flying at inner area changes much more bigger than others far away from the GS; even they have the same altitude and speed. However, according to Figure 4, the AS node locates at inner area; for example, $R = 50$ km. It is less sensitive to AoA errors than those located in the edge of the macrocell; for example, $R = 200$ km. Therefore, the tolerance of AoA deviations can be roughly estimated, when $\Delta \leq 0.1\Delta_{\max}$, the performance becomes negligible ($\delta_{\text{SINR}} \leq 3$ dB, as shown in Figure 4). By using macrocell model illustrated in Figure 1, the AoA deviations can be expressed in terms of the position drift, denoted by δ_x, which is given by

$$\tan(\theta_m \pm \Delta) = \frac{x \pm \delta_x^{\pm}}{h_a}, \tag{28}$$

where x denotes the horizontal distance between AS-m and the GS, and

$$\delta_x^+ = h_a\left(\tan\left(\theta_m + \Delta\right) - \tan\left(\theta_m\right)\right),$$
$$\delta_x^- = h_a\left(\tan\left(\theta_m\right) - \tan\left(\theta_m - \Delta\right)\right). \quad (29)$$

It is noteworthy that the position tolerance for beamforming is quite different between inner and boundary areas of a macrocell. With $M = 10$, for example, we have $\Delta_{\max} = 0.2014$ rad (11.5394°). For the case of $R = 200$ km, $\theta_{\max} = 1.5208$ rad, and $\theta_{\min} = 0$ rad, it can be shown that

$$\begin{aligned}\delta_{\max}^+ &= h_a\left(\tan\left(\theta_{\max} + 0.1\Delta_{\max}\right) - \tan\left(\theta_{\max}\right)\right)\\ &= 134.9898\,\text{km},\\ \delta_{\max}^- &= h_a\left(\tan\left(\theta_{\max}\right) - \tan\left(\theta_{\max} - 0.1\Delta_{\max}\right)\right)\\ &= 57.5024\,\text{km},\\ \delta_{\min}^+ &= \delta_{\min}^- = h_a\left(\tan\left(0.1\Delta_{\max}\right)\right)\\ &= 0.2014\,\text{km}.\end{aligned} \quad (30)$$

Apparently, with the position drift $\delta_{\min}^+$, that is, approximately 200 meters, for a turbine powered jetliner or a corporate jet cruising at 450–500 Knots in general, which is 231.3–257.2 meters per second, one AS node should update its position no more than 1 second. Note that the updating frequency can be lower at the edge of a macrocell, which will result in a less burden in implementation.

Based on the promising A/G datalink protocols (i.e., L-DACS1 and L-DACS2), it is required that every AS should feedback its position or distance away from the GS in every superframe [24, 34]. Note that the superframe duration is 0.24 second in L-DACS1 or 1 second in L-DACS2, which means the feedback channel is already designed in future systems and the updating frequency will also fulfill all requirements of the proposed aeronautical SDMA system.

5. Numerical Results

In this section, numerical results are presented under assumptions that the unitary noise variance $\sigma^2 = 1$, the standard ULA with $d = 0.5\,\lambda$, the path-loss exponent $n = 2.0$, and the close-in reference distance $l_0 = 1$ m.

Figure 5 shows the SDMA gain versus total number of AS nodes K for different number of antenna elements M, where 10^6 Monte Carlo simulations are carried out to plot each point. It demonstrates that with the overall AS nodes number K increased, the performances of SDMA is improved, which is termed as the multiuser diversity. On the other hand, higher SDMA gain can also be obtained by employing large M, where the dimension of ARVs is extended to enhance the performance of SDMA. Hence, we can conclude that the system capacity can be improved by increasing the number of antenna elements and the number of aircraft, theoretically. Besides, comparing with the OBF under the same SINR constraint, the proposed ZFBF-MFS algorithm could obtain apparent advantages.

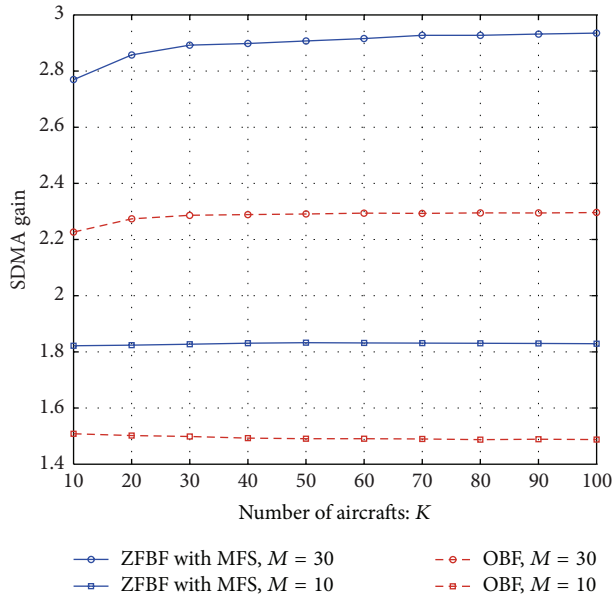

Figure 5: The SDMA gain versus total number of AS nodes K.

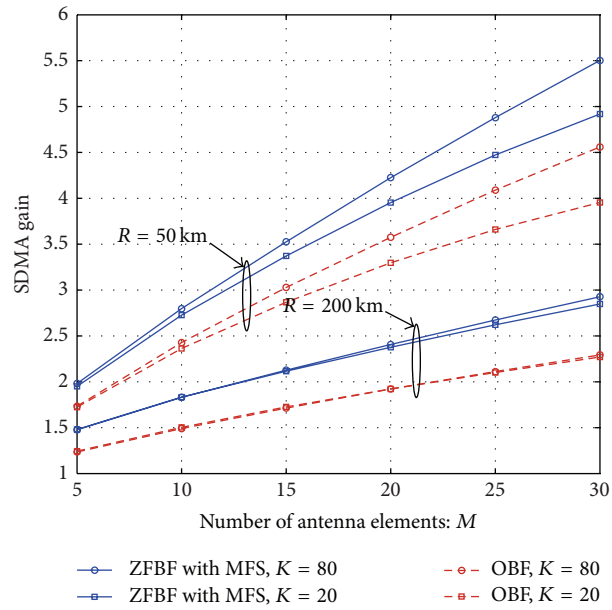

Figure 6: The SDMA gain comparison of increasing number M of antenna elements in the different macrocell, where $R = \{50, 200\}$.

Simulation results of SDMA gain versus number of antenna elements (M) are presented in Figure 6, where $R = \{50, 200\}$ (in km) are considered. It shows that the SDMA gain can be strongly improved by increasing the number of antenna array elements, since the orthogonality between different AS nodes can be improved by employing more array elements. It also shows that the performance gap is limited between the systems with different values of overall AS nodes K. In this case, the number of antennas becomes the main factor of SDMA gain when a practical density of aircraft environment is considered in a macrocell, for example,

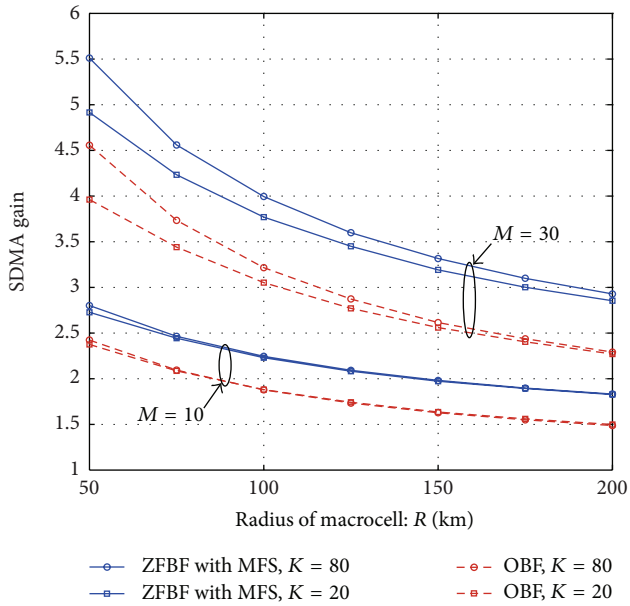

Figure 7: SDMA gain as a function of R, where $M = \{10, 30\}$.

less than a hundred. Note that the OBF with the same SINR constraint also has the same increasing trend but lower performance.

In Figure 7, simulation results of our proposed primary rate guaranteed SDMA and OBF with SINR constraints are presented with different array elements numbers; that is, $M = \{10, 30\}$. It shows that the SDMA gain degrades as R increases. If the location of AS follows the uniform distribution in a macrocell, more AS nodes will result in similar AoAs when the radius of macrocell increases. The detailed AoA distribution could be found in [35]. Consequently, we can observe that the SDMA strategy becomes efficient as the macrocell is relatively small. Furthermore, the performance gaps between $K = 80$ and $K = 20$ are insignificant, which indicates the proposed SDMA approach is able to provide stable performance with different K.

In general, the simulations above illustrate that the proposed ZFBF with MFS is a proper SDMA approach for 4DT services. And the ZFBF with MFS will obtain a better SDMA gain compared with OBF in [19, 20, 35].

6. Conclusion

In this paper, an SDMA-based aeronautical M2M communication system has been proposed together with a low complexity user selection approach. It has been shown that a primary rate is guaranteed for all selected AS nodes, while the same frequency spectrum can be reused by ZFBF. Using the proposed matrix-inverse free user selection, the SINR of each AS candidate is calculated with acceptable complexity, that is, $\mathcal{O}(KM^2)$.

Through simulations, we have confirmed that the SDMA gain can be strongly improved by increasing the number of antenna elements, while the SDMA can be more efficient when the radius of macrocell is relatively small. Furthermore, our proposed SDMA approach is able to provide stable performance in a high density AS nodes scenario, which is desired by the future aeronautical SMN-M2M communications.

Acknowledgments

This work was supported by the National Natural Science Foundation of China (Grant nos. 61250001, 91338106, 61231011, 61171069, and 61231013) and by the National High Technology Research and Development Program (Grant no. 2011AA110102).

References

[1] International Civil Aviation Organization, "Global air navigation capacity & efficiency plan," in *Proceedings of the 12th Air Navigation Conference (ANC '12)*, vol. 9750, Montreal, Canada, 2012.

[2] SESAR, *System Interoperability With Air/Ground Data Sharing*, European ATM Master Plan, 2nd edition, 2012.

[3] International Civil Aviation Organization, "Data communication issues," in *Proceedings of the 12th Air Navigation Conference (ANC '12)*, AN-conf/12-WP37.1.1, Montreal, Canada, 2012.

[4] EUROCONTROL, *Initial 4D- 4D Trajectory Data Link (4DTRAD) Concept of Operations*, 1st edition, 2008.

[5] S. Plass, "Seamless networking for aeronautical communications: one major aspect of the SANDRA concept," *IEEE Aerospace and Electronic Systems Magazine*, vol. 27, no. 9, pp. 21–227, 2012.

[6] M. Schnell and S. Scalise, "NEWSKY: concept for networking the sky for civil aeronautical communications," *IEEE Aerospace and Electronic Systems Magazine*, vol. 22, no. 5, pp. 25–29, 2007.

[7] International Civil Aviation Organization, *Global Operational Data Link Document (GOLD)*, 1st edition, 2010.

[8] SESAR, "I-4D- flying a new dimension," SESAR Factsheet, 2012.

[9] M. R. C. Jackson, J. Gonda, R. Mead, and G. Saccone, "The 4D trajectory data link (4DTRAD) service: closing the loop for air traffic control," in *Proceedings of the Integrated Communications, Navigation and Surveillance Conference (ICNS '09)*, pp. 1–10, Arlington, Va, USA, May 2009.

[10] EUROCONTROL, "Air traffic requirements," EEC Note No. 28/98, 1998.

[11] N. Neji, R. D. Lacerda, A. Azoulay, and T. Letertre, "Survey on the future aeronautical communication system and its development for continental communications," *IEEE Transactions on Vehicular Technology*, vol. 62, no. 1, pp. 182–1191, 2013.

[12] R. Jain and F. Templin, "Requirements, challenges, and analysis of alternative for wireless datalinks for unmanned aircraft systems," *IEEE Journal on Selected Areas in Communications*, vol. 30, no. 5, pp. 852–860, 2012.

[13] International Civil Aviation Organization, "Report on the results of the International Telecommunications Union (ITU) World Radiocommunication Conference (WRC '12)," in *Proceedings of the 12th Air Navigation Conference (ANC '12)*, AN-conf/12-IP/7, Montreal, Canada, 2012.

[14] International Civil Aviation Organization, "Air traffic management," ATM 501, 2007, No. 4444, 15th edition.

[15] J. Choi, *Optimal Combining and Detection: Statistical Signal Processing for Communications*, Cambridge University Press, 2010.

[16] H. van Trees, *Optimum Array Processing, Part IV of Detection, Estimation, and Modulation Theory*, Wiley-Interscience, New York, NY, USA, 2002.

[17] D. C. Chang and C. N. Hu, "Smart antennas for advanced communication systems," *Proceedings of IEEE*, vol. 100, no. 7, pp. 2233–2249, 2012.

[18] G. Caire and S. Shamai, "On the achievable throughput of a multiantenna Gaussian broadcast channel," *IEEE Transactions on Information Theory*, vol. 49, no. 7, pp. 1691–1706, 2003.

[19] J. Choi and J. Ha, "Orthogonal beamforming for overlay mode of OFDMA-based rural broadband wireless access," in *Proceedings of the IEEE Wireless Communications and Networking Conference: PHY and Fundamentals (WCNC '12)*, pp. 508–512, 2012.

[20] J. Xie, J. Zhang, and L. Bai, "Multilayer orthogonal beamforming for priority-guaranteed wireless communications," *International Journal of Distributed Sensor Networks*, vol. 2012, Article ID 307467, 8 pages, 2012.

[21] T. Yoo, G. J. Foschini, R. A. Valenzuela, and A. J. Goldsmith, "Common rate support in multi-antenna downlink channels using semi-orthogonal user selection," *IEEE Transactions on Information Theory*, vol. 57, no. 6, pp. 3449–3461, 2011.

[22] T. Yoo and A. Goldsmith, "On the optimality of multiantenna broadcast scheduling using zero-forcing beamforming," *IEEE Journal on Selected Areas in Communications*, vol. 24, no. 3, pp. 528–541, 2006.

[23] F. Hoffmann, U. Epple, M. Schnell, and U. Fiebig, "Feasibility of LDACS1 cell planning in European airspace," in *Proceedings of the IEEE/AIAA 31st Digital Avionics Systems Conference (DASC '12)*, Williamsburg, Va, USA, October 2012.

[24] EUROCONTROL, "L-DACS1 system definition proposal deliverable D2," Tech. Rep, 2009.

[25] E. Haas, "Aeronautical channel modeling," *IEEE Transactions on Vehicular Technology*, vol. 51, no. 2, pp. 254–264, 2002.

[26] D. Stacey, *Aeronautical Radio Communication Systems and Networks*, Wiley, 2008.

[27] W. L. Stutzman and G. A. Thiele, *Antenna Theory and Design*, John Wiley & Sons, New York, NY, USA, 1981.

[28] G. M. Galvan-Tejada and J. G. Gardiner, "Theoretical model to determine the blocking probability for SDMA systems," *IEEE Transactions on Vehicular Technology*, vol. 50, no. 5, pp. 1279–1288, 2001.

[29] Q. H. Spencer, A. L. Swindlehurst, and M. Haardt, "Zero-forcing methods for downlink spatial multiplexing in multiuser MIMO channels," *IEEE Transactions on Signal Processing*, vol. 52, no. 2, pp. 461–471, 2004.

[30] M. Kountouris and J. G. Andrews, "Downlink SDMA with limited feedback in interference-limited wireless networks," *IEEE Transactions on Wireless Communications*, vol. 11, no. 8, pp. 2730–2741, 2012.

[31] H. Li, Y.-D. Yao, and J. Yu, "Outage probabilities of wireless systems with imperfect beamforming," *IEEE Transactions on Vehicular Technology*, vol. 55, no. 5, pp. 1503–1515, 2006.

[32] A. Elnashar, S. M. Elnoubi, and H. A. El-Mikati, "Further study on robust adaptive beamforming with optimum diagonal loading," *IEEE Transactions on Antennas and Propagation*, vol. 54, no. 12, pp. 3647–3658, 2006.

[33] V. Vakilian, J.-F. Frigon, and S. Roy, "Effects of angle-of-arrival estimation errors, angular spread and antenna beamwidth on the performance of reconfigurable SISO systems," in *Proceedings of the 13th IEEE Pacific Rim Conference on Communications, Computers and Signal Processing (PACRIM '11)*, pp. 515–519, August 2011.

[34] EUROCONTROL, "L-DACS2 system definition proposal: deliverable D2," Tech. Rep, 2009, Version 1.0.

[35] "Dual priority SDMA in aeronautical communications," in *Integrated Communications, Navigation and Surveillance Conference (ICNS '13)*, pp. 1–49, Herndon, Va, USA, April 2013.